Motion and Attitude Estimation Using Inertial Measurements with Complementary Filter

Stephen P. Tseng Wen-Lung Li Chih-Yang Sheng Jia-Wei Hsu
Institute of Mechatronic Engineering
National Taipei University of Technology
Taipei, Taiwan, ROC
stephen@ntut.edu.tw

***Abstract*—This study has utilized the advantages of inertial sensors and complementary filter to estimate the motions and attitudes. Although the progress in micro-electro-mechanical systems(MEMS) has improved the qualities of the inertial sensors, such as accelerometers and gyroscopes, their bandwidths limit them from accurate measurements and applications. However, by using the complementary filter properly, the signals can be adopted to generate reliable data for positioning. The frequency response and transfer to obtain the functions best results, of sensors are identified and the cut-off frequency of complementary filter is defined accordingly. To minimize the measurement error caused by the external forces and disturbances, a state estimator has been integrated into the system. Tests are conducted on linear and rotating platforms to validate the real-time performance of this system. The estimated data proves the functionality of this developed complementary filter to blend the high-frequency measurements of gyroscopes and low-frequency ones of accelerometers to generate trustworthy positioning information.**

Keywords-inertial measurement; complementary filter; motion estimation

I. INTRODUCTION

The inertial measurements are widely used in the traditional avionic systems before the emergence of Global Positioning System (GPS). They are still playing important roles in those fields which GPS is not a candidate of positioning measurement, such as submerged vehicle and in-door positioning. Inertial Measurement Unit (IMU) is always the first candidate as the redundant measurement in the event of GPS failure. While GPS relies on the signals from the satellite in the space, which can be interfered or blocked by external objects, the IMU always generates signals of vehicle motions independently.

It has been understood that the noise is the major problem in the IMU applications. As the positions and attitudes both are generated by the 1st or 2nd integration of the measurements, drifting and pulsating noises will create uncontrollable errors in the calculation. Researches and studies of eliminating these measured errors have never stopped. Mahony [1] has proposed a combination of two nonlinear complementary filters to improve the calculation of unmanned helicopter attitudes interfered by the noise of gyroscope signals. Rehbinder [2] and Martin [3] have adopted the state observer and Kalman filter to minimize the error in nonlinear rotating motions. Jurman [4] and Zhu [5] have utilized MEMS Attitude and Heading Reference System (AHRS) and Kalman filter to estimate the attitudes. Euston [6] has adopted the complementary filter, IMU and airspeed sensor for attitude estimation. Vasconcelos [7] proposed a discrete time-varying complementary filter to compensate the error caused by gyroscope measurement. Hong [8] has designed a fuzzy algorithm to compensate the error.

In general, accelerometer and gyroscope are the basic sensors to measure the linear acceleration and rotating speed respectively. In certain applications, magnetomemter is also required to locate the magnetic north of earth and secondly form a supplementary orientation along with the use of gravity. To take advantages of them, this study has adopted the structure of complementary filter [1] and enhanced the performance by the passive filter proposed in [Mahony] to minimize the error caused by interfered measurements. The designed complementary filter is tested to estimate motions on linear and rotating platforms. The results have shown that the performance of the developed algorithm outperforms the commercial counterpart.

II. CHARATERISTICS OF INERTIAL SENSORS

Generally, without any external force, accelerometers are used to measure the projected gravity force on each axis and the angular position can be calculated via trigonometric functions. However, this approach only can be applied to low frequency of motions because most of the MEMS design cannot generate accurate and un-disturbed high frequency signals. Furthermore, using gravity to estimate the attitude will prevent the calculation of yaw angle (heading). The earth magnetic field, measured by the magnetomemter, is used to resolve this singularity commonly.

To accommodate this high frequency motions, gyroscope is adopted to measure the angular velocity so that relative angular motion can be obtained by integration. Unfortunately, this integration usually mixes with low frequency drifting and biased signals such that the results tend to diverge even if the sensor is stationary. This drawback prevents the gyroscope from being the primary sensor for attitude estimation.

Identify applicable sponsor/s here. *(sponsors)*

III. ESTIMATION OF ATTITUDES

The most popular motion system used is the Euler angles, which defines the attitudes of an entity by yaw (ψ), pitch(θ) and roll(φ) angles, in the specific sequence of rotation with respect to Z, Y and X axes of a referred coordinate system. In general, the X, Y and Z axes of the inertial coordinate system are defined as North, East and Downward directions and Abbreviated as the NED coordinate. The directions of the rotated entity, usually are called the body coordinate, are defined by the Euler angles. The conformation of Euler angles between the inertial and body coordinates are shown in Figure1.

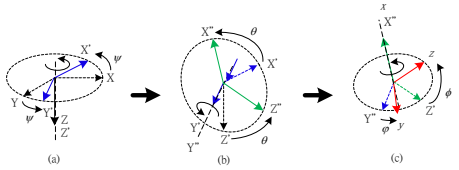

Figure 1. Conformation of Euler angles between the inertial and body coordinates

Then the transformation between the inertial and body coordinates can be defined by a matrix calculation as

$$\begin{bmatrix} X \\ Y \\ Z \end{bmatrix} = \begin{bmatrix} C_\psi C_\theta & -S_\psi C_\phi + C_\psi S_\theta S_\phi & S_\psi S_\phi + C_\psi S_\theta C_\phi \\ S_\psi C_\theta & C_\psi C_\phi + S_\psi S_\theta S_\phi & -C_\psi S_\phi + S_\psi S_\theta C_\phi \\ -S_\theta & C_\theta S_\phi & C_\theta C_\phi \end{bmatrix} \begin{bmatrix} x \\ y \\ z \end{bmatrix} \quad (1)$$

Where C_i is cos(i) and S_j is sin(j). Since the referred inertial signals are the gravity and earth magnetic flux, which can be defined as vectors in the Downward and North directions, i.e. Z and X axes.

The relationship between the measured signals on each axis of sensor in the body coordinate and the referred signals projected can be defined by the directional cosine, which states that any vector defined in two coordinate systems can be related as

$$\begin{bmatrix} \mathrm{X} \\ \mathrm{Y} \\ \mathrm{Z} \end{bmatrix} = \begin{bmatrix} \cos(\theta_{Xx}) & \cos(\theta_{Xy}) & \cos(\theta_{Xz}) \\ \cos(\theta_{Yx}) & \cos(\theta_{Yy}) & \cos(\theta_{Yz}) \\ \cos(\theta_{Zx}) & \cos(\theta_{Zy}) & \cos(\theta_{Zz}) \end{bmatrix} \begin{bmatrix} x \\ y \\ z \end{bmatrix} \quad (2)$$

where cos(θ_{ij}) is the cosine of the angle between the I axis of inertial coordinate and the j axis of body coordinate. Alternatively, the directional cosine matrix also defines the transformation between the inertial and body coordinates. Thus, the Euler angles can be estimated by using the projected vectors of gravity and earth magnetic flux measured by the accelerometers and magnetic sensors.

Hence, by normalizing the measurements of gravity and comparing the elements in the transformation matrix of Euler and directional cosine, the pitch and roll angles can be found as

$$\theta = \sin^{-1}(-\cos\theta_{zu}) = \sin^{-1}(-g_x) \quad (3)$$

$$\phi = \tan^{-1}\left(\frac{\cos\theta_{zv}}{\cos\theta_{zw}}\right) = \tan^{-1}\left(\frac{g_y}{g_z}\right) \quad (4)$$

where g_x, g_y and g_z are the normalized measured gravity on each axis in the body coordinate. Similarly, the yaw angle can be found by using the normalized earth magnetic flux measurements in the body coordinate as

$$\psi = \tan^{-1}\left(\frac{m_y\cos(\phi) - m_z\sin(\phi)}{m_x\cos(\theta) + m_y\sin(\theta)\sin(\phi) + m_z\sin(\theta)\cos(\phi)}\right) \quad (5)$$

where m_x, m_y and m_z are the normalized measured earth magnetic flux on each axis in the body coordinate.

IV. COMPLEMENTARY FILTERING

Although the above-mentioned equations can be used to estimate the attitudes of an entity, the characteristics of the sensors make the calculation valid only in the low frequency of motion. To verify the dynamic range of sensors, the frequency responses are measured experimentally for the Xsens MTi IMU used in this study, the results of accelerometer and magnetomemter are shown in Figure 2 and 3. Both sensors showed good dynamic response to the low frequency motions but the accelerometer would diverge, while the magnetic sensor would decay, in the high frequency.

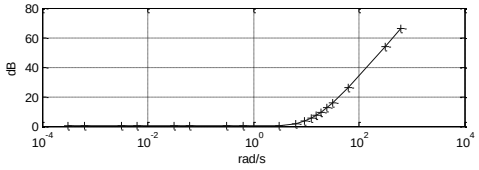

Figure 2. Dynamic response of accelerometer

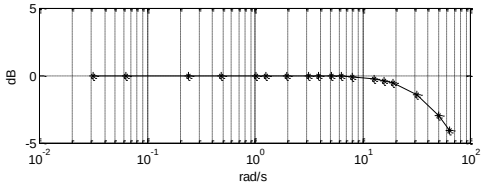

Figure 3. Dynamic response of magnetometer

On the other hand, the dynamic response of gyroscope, shown in Figure 4, has better fidelity in the high frequency but poor quality in the low frequency range.

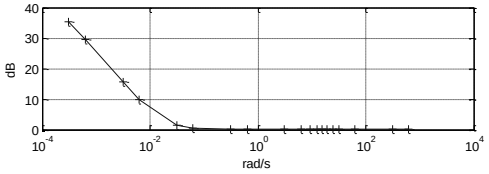

Figure 4. Dynamic response of gyroscope

However, as the reliable frequency ranges of these sensors have overlapped and covered the whole range, the complementary filtering [9] emerges as the best candidate to estimate the attitudes in the dynamic motions.

To utilize the best performance of each sensor, the complementary filtering is designed to extract the low

frequency of the accelerometer/magnetomemter and the high frequency of gyroscope as shown in Figure 5. Based on the measured frequency response of sensors shown in Figure 2~4, the dynamic response of sensors can be modeled as

$$G_A(s) = (0.1s+1)(0.05s+1) \tag{6}$$

$$G_M(s) = \frac{50.265}{s+50.265} \tag{7}$$

$$G_G(s) = \frac{s+0.0185}{s} \tag{8}$$

for accelerometer, magnetomemter and gyroscope respectively.

To obtain the best estimation of the attitudes, the break frequencies of the low/high pass filters must be carefully defined to keep the valid signals while be capable of suppressing the unwanted noisy response of sensors. After carefully examination of the sensors' dynamic models, the break frequency of low-pass filter was chosen at 2.5 rad/s for accelerometer and magnetometer. The break frequency of high-pass filter for gyroscope was selected at 3.3 rad/s such that the best comprehensive performance of the complementary filter is obtained. Furthermore, because the divergence of each sensor is approximated differently, the final low pass filters for accelerometer and magnetometer were chosen as

$$G_{LA}(s) = \frac{1}{0.063s^3 + 0.475s^2 + 1.1937s + 1} \tag{9}$$

$$G_{LM}(s) = \frac{1}{0.3979\mathrm{s} + 1} \tag{10}$$

respectively. The high-pass filter for gyroscope was defined as

$$G_H(s) = \frac{s^2}{s^2 + 0.6s + 0.09} \tag{11}$$

To verify the effectiveness of this complementary filter, simulations on Matlab have been conducted. A frequency sweep test was done for the designed filtering. With the sensors modeled by the transfer function shown in Eq. 6~8 and the low/high pass filter modeled as Eq. 9~11, the designed complementary filter response is shown in Figure 6 for signals from accelerometer and gyroscope. The filtered response for signals from the magnetometer and gyroscope is shown in Figure 7. In both cases, unity response can be seen except in a small range where the gain and phase error are minimized. An additional compensation is added to further reduce the error, in which the inverse transfer function of Figure 6 and 7 is used.

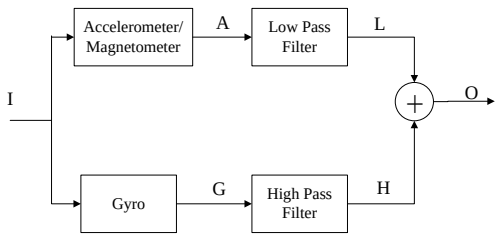

Figure 5. Complementary filter for IMU

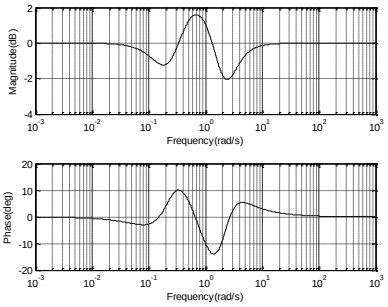

Figure 6. Simulated frequency response of complementary filtering of accelerometer and gyroscope outputs

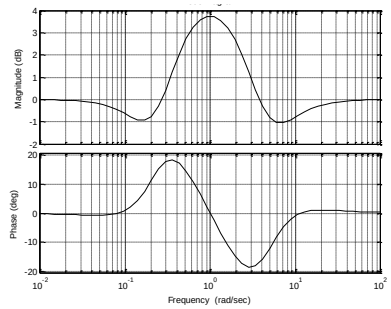

Figure 7. Simulated frequency response of complementary filtering of magnetometer and gyroscope outputs

V. ADAPTIVE COMPLEMENTARY FILTER

The most important assumption up to this point is that no external force is applied to the system. When external load is applied, the measurements from the accelerometer would be interfered by the acceleration created by the external forces. To minimize the error caused by the interfered signal, a passive complementary filter developed by Mahony [1] is adopted. The processing of this passive complementary filter is shown in Figure 8. Generally, the signal from gyroscope will dominate the calculation to minimize the effects of biased acceleration signal. Thus, if the overall measured force in the accelerometer is greater or less than the magnitude of gravity, exceeding a tolerance, the passive complementary filter will be selected to estimate the attitude. With this enhancement, the developed system can calculate the attitude of a moving object no matter if external force exists or not.

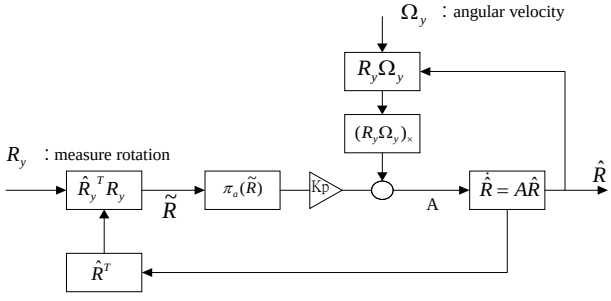

Figure 8. Passive Complementary Filter [1]

VI. EXPERIMENTS AND RESULTS

To verify the performance of the designed complementary filter, various experiments are conducted and results are compared with the commercial products.

A. Hardware

The inertial measurement unit used in this study is the Xsens MTi integrated IMU. It can output the measured 3-axis accelerations, magnetic flux and angular velocities. This IMU has an onboard processor so that estimated attitudes are also output for reference which is used for comparison to check the performance of the developed algorithm. The key specifications of this IMU are listed in Table I.

TABLE I. SPECIFICATIONS OF IMU SENSORS

Sampling Rate		30 (Hz)
Measurement Range	Accelerometer	±5 (G)
	Gyroscope	±300 (deg/s)
	Magnetometer	±750 (mGauss)

Other than the static equivalent condition, forced linear and rotating motions are applied to the unit in order to verify the robustness of the complementary filter. To generate rotating motion, a dual-axis rotating platform powered by AC servo motors is used. The actual rotation of the platform is measured by optical encoders whose resolution is 0.036°. The motion of the platform is commanded by PWM signals and recorded together with the measurements from the IMU for post-processing. The experiment apparatus is shown in Figure 9. To verify the performance in dual-axis motion, an inclined block is inserted underneath the IMU, as shown in Figure 10.

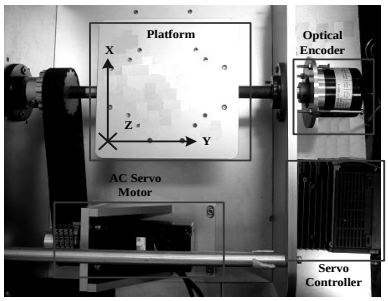

Figure 9. Experimental apparatus of rotating motion

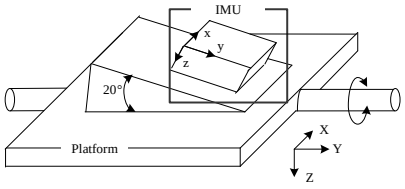

Figure 10. Dual-axis experimental apparatus of rotating motion

The linear motion is generated by a ball screw driver controlled by an AC servo motor. The linear motion is measured by a laser range finder which has a resolution of 1μm. The apparatus of linear motion platform is shown in Figure 11.

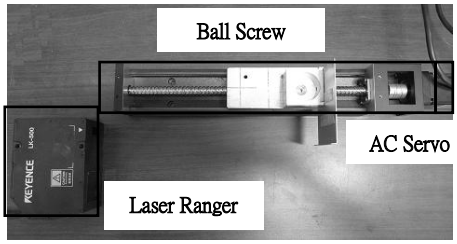

Figure 11. Experimental apparatus of linear motion

B. Experiments

Various experiments are designed to check the performance of the developed complementary filtering algorithm. All these tests are designed to check the performance of the system with or without external force, including:

(1) Single-axis sinusoidal rotating motion

(2) Dual-axis sinusoidal rotating motion

(3) Single-axis step rotating motion

(4) Single-axis linear acceleration/deceleration

(5) Offset single-axis sinusoidal rotating motion

C. Results

1) Single-axis sinusoidal rotating motion

In this experiment, the platform was driven to make a ±10° rotation at various frequencies in the pitch axis. The results of estimated measurements of accelerometer, magnetometer and gyroscope were collected and plotted as a frequency diagram as shown in Figure 12. It is obviously that the developed complementary filtering algorithm performed better than the counterparts from the commercial IMU. The gain error is less than 1 dB in all the range of experiment.

2) Dual-axis sinusoidal rotating motion

At this stage, a 20° inclination was added to the IMU so that the system is under dual-axis rotating motion in the body coordinate. However, since the platform is actually rotated along the pitch axis as shown in Figure 10. The results are shown in Figure 13 which shows that the developed complementary filter can make better estimation than the onboard processor in the IMU.

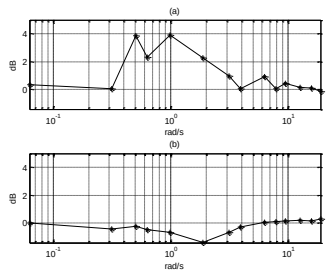

Figure 12. Frequecy response of single-axis pitch rotation. (a) MTi IMU (b) developed complementary filter

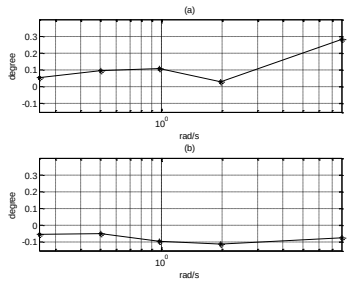

Figure 13. Estimation errors of dual-axis pitch rotation. (a) MTi IMU (b) developed complementary filter

3) Single-axis step rotating motion

The step response is checked to understand the transient response of the estimation to ensure the measurement under rapid motions. The testing data is shown in Figure 14. Comparing with the actual rotation measured by the optical encoder, the estimation made by the developed complementary filter tracked the actual motion with little error in real-time, while the estimation produced not only delayed but also with noticeable error by the commercial IMU. The settling time of the response from the commercial IMU is also far greater than the developed algorithm. For various sizes of step command, the settling time is drawn in Figure 15

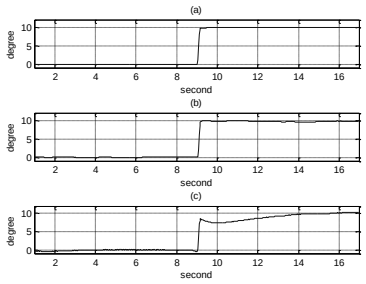

Figure 14. Step response of the IMU and developed complementary filter. (a) Actual motion, (b) Estimation with complementary filter, and (c)Ouput from IMU

Also tested is the steady-state error for various sizes of step command. In Figure 16, the developed algorithm also performed better than the commercial counterpart.

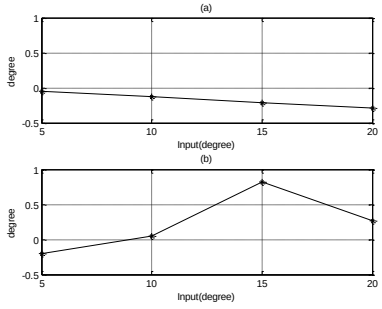

Figure 15. Steady-state errors for various sizes of step motions, (a) Estimation by complementary filter (b) Estimation by IMU

TABLE II. PITCH ANGLE ESTIMATION ERRORS IN SINGLE-AXIS LINEAR MOTION

Axis of Rotation	Angle	Maximum Error		Standard Deviation	
		IMU	ACF	IMU	ACF
Z	0	0.7946	2.9243	0.3091	1.2044
	30	0.6822	0.9573	0.2555	0.2284
	60	1.9537	0.6650	0.5911	0.1741
	90	2.4400	0.3186	0.6739	0.0951
Y	0	0.5413	0.8299	0.2092	0.1950
	30	0.7801	1.8780	0.2907	0.5182
	60	1.1541	2.9196	0.4145	0.9782
	90	3.7047	4.9681	1.0689	2.4624
X	0	0.6476	0.9721	0.2680	0.2652
	30	0.7953	1.5259	0.2717	0.3820
	60	0.7735	2.1546	0.2398	0.4822
	90	0.9457	2.7678	0.2560	0.8448

TABLE III. ROLL ANGLE ESTIMATION ERRORS IN SINGLE-AXIS LINEAR MOTION

Axis of Rotation	Angle	Maximum Error		Standard Deviation	
		IMU	ACF	IMU	ACF
001	0	2.4102	0.4847	0.6340	0.1934
	30	1.9444	0.5074	0.5959	0.1200
	60	2.2720	0.5004	0.6620	0.1480
	90	0.6130	0.7756	0.2008	0.1783
010	0	2.8781	0.2689	0.8359	0.0783
	30	3.5206	0.3162	1.0953	0.0951
	60	4.9377	1.3076	1.5045	0.4531
	90	30.1806	22.9074	8.9577	7.7561
100	0	2.9873	0.4701	0.9500	0.1744
	30	2.2363	1.2799	0.6465	0.3530
	60	1.8046	2.7740	0.5439	0.7084
	90	2.1066	4.3171	0.6320	1.1582

4) Single-axis linear acceleration/deceleration

In this test, the IMU unit was placed at different angles form the direction of motion to validate the calculation of attitudes. The motion of linear platform is defined as shown in Figure 16. The estimated pitch and roll angles of the object are listed in Table II and III for various positioning angles in different axes. In most of the tests, the developed complementary filter made better estimation than the commercial IMU with no surprise. However, it is worth to notice that, in Table III, when the IMU was positioned 90°, the estimations made by the developed algorithm and the commercial unit both grow dramatically. This error is caused by a phenomenon called Gimbals Lock, in which calculation of Euler angle is close to a singularity.

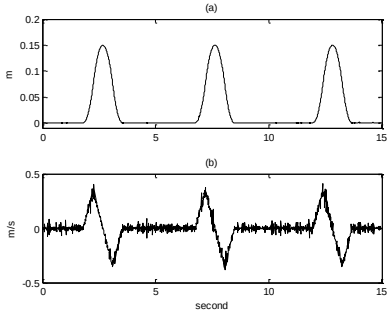

Figure 16. Testing pattern for linear motion, (a) displacement, (b) velocity

TABLE IV. PITCH ANGLE ESTIMATION ERRORS IN DUAL-AXIS LINEAR MOTION

Axis of Rotation	Angle	Maximum Error		Standard Deviation	
		IMU	ACF	IMU	ACF
Z	0	4.3071	1.7219	1.3842	0.5440
	30	3.5302	1.6213	1.1463	0.4923
	60	3.6993	1.8748	1.4811	0.7177
	90	3.7866	1.8967	1.4796	0.5591
Y	0	4.3122	1.4873	1.4236	0.4603
	30	4.1181	1.8910	1.3867	0.6506
	60	4.0328	2.7632	1.4467	1.0037
	90	4.3686	3.8901	1.7465	1.2158
X	0	3.9950	1.2664	1.1544	0.4252
	30	3.9731	1.5409	1.2315	0.4910
	60	3.1914	1.5917	1.1350	0.5241
	90	3.1886	1.4526	0.6994	0.4873

TABLE V. ROLL ANGLE ESTIMATION ERRORS IN DUAL-AXIS LINEAR MOTION

Axis of Rotation	Angle	Maximum Error		Standard Deviation	
		IMU	ACF	IMU	ACF
001	0	3.2542	1.3671	0.9924	0.4873
	30	3.0097	1.5912	1.0018	0.4652
	60	2.9064	1.8768	0.9104	0.6021
	90	3.6021	1.6993	1.0579	0.5601
010	0	3.0322	1.5521	0.9250	0.4386
	30	3.4478	1.7645	1.0946	0.5246
	60	6.0854	5.3143	2.0282	1.6033
	90	32.6870	43.6478	9.2769	20.4322
100	0	3.3546	1.3996	1.2287	0.4160
	30	3.9174	1.5104	1.3013	0.4718
	60	3.5856	2.6981	1.4242	0.7233
	90	4.3175	4.0465	1.4427	0.9819

5) Offset single-axis sinusoidal rotating motion

A 20cm offset is added to the IMU in the 0.4Hz sinusoidal yaw rotating motion in this test. This offset will create centrifugal and Coriolis forces on the measurements other than the gravity. Estimation of one case, no inclination and 0° pitch, is shown in Figure 17 and the developed complementary filtering algorithm produced less error than the commercial one. Results of all other cases are listed in Table IV and V. In most of the cases, the developed complementary filter performs better than the commercial IMU. Notice that the Gimbals Lock happened in this experiment, too.

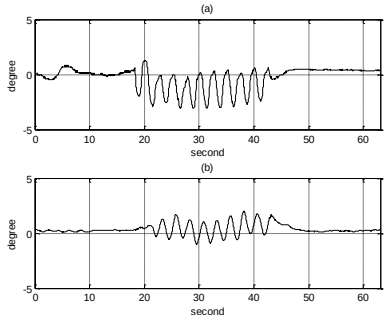

Figure 17. Pitch angle estimation errors in an offset rotation

VII. CONCLUSIONS

This study has developed an adaptive complementary filter for estimating attitudes of moving object using measurements from an IMU. The developed algorithm has been simulated and proper compensation was added to improve the performance. Various experiments are conducted to validate the functionality of this developed system and the results show that the developed means outperforms those from the commercial IMU. By applying this complementary filtering algorithm, the signals measured by accelerometer, magnetometer and gyroscope can be blended wisely and properly to estimate the actual attitudes of a moving object accurately. This estimation can be used to augment the accuracy of GPS system or be a substitution when GPS signal is invalid.

The Gimbals Lock phenomenon was also noticed in the experiment which would prevents the developed algorithm from estimation in certain conditions. This issue could be resolved by using Quarterion instead of directional cosine matrix. However, the performance and capability of the complementary filter have been validated for future applications without any doubt.

ACKNOWLEDGMENT

This study was conducted under the funding supported by National Science Council of Taiwan, Project: NSC 97-2752-E-027-002-PAE and 98-2752-E-027-001-PAE. The authors appreciate all supports from National Science Council of Taiwan and its staff.

REFERENCES

[1] R. Mahony, T. Hamel and Jean-Michel Pflimlin,"Nonlinear Complementary Filters on the Special Orthogonal Group," IEEE Transactions on Automatic Control, vol. 53, pp. 1203-1218, 2008.

[2] H. Rehbinder and X. Hu, "Nonlinear Pitch and Roll Estimation for Walking Robots," IEEE International Conference on Robotics and Automation, vo1.3, pp.2617-2622, 2000.

[3] P. Martin and E. Salaün, "A General Symmetry-Preserving Observer for Aided Attitude Heading Reference Systems, " Decision and Control, CDC 2008, 47h IEEE Conference, pp.2294-2301,2008.

[4] D. Jurma n, M. Ja nkovec, R. Ka mnik and M.Topic., " Calibration and Data Fusion Solution for the Miniature Attitude and Heading Reference System," Sensors and Actuators, A-Physical, vol. 138, pp.411-420, 2007.

[5] R. Zhu , D . Sun , Z. Zhou and D. Wang, "A Linear Fusion Algorithm for Attitude Determonation Using Low Cost MEMS-Based Sensors , " Measurement: Journal of the International Measurement Confederation , vol. 40,pp.322-328, 2007.

[6] M. Euston, P. Coote, R. Mahony, J. Kim and T, Hamel "A Complementary Filter for Attitude Estimation of a Fixed-Wing UAV with a Low-Cost IMU, " 6 th International Conference on Field and Service Robtics, pp.340-345, 2008.

[7] J.F. Vasconcelos, C. Silvestre, P. Oliveira, P. Batista and B. Cardeira, "Discrete Time-Varying Attitude Complementary Filter," American Control Conference, pp.4056-4061, 2009.

[8] S. K. Hong, "Fuzzy Logic Based Closed-Loop Strap Down Attitude System for Unmanned Aerial Vehicle (UAV)," Sensors and Actuator A: Physical, vol. 107, pp.109-118, 2003.

[9] R. P. G. Collinson, Introduction to Avionics. Microwave Technology Series 11, Chapman & Hall, 1st, pp.231-237, 1996.